Searches for Exotic Processes in Double Beta Decay with EXO-200

T.N. JOHNSON
Indiana University Center for Exploration of Energy and Matter
2401 Milo B. Sampson Lane
Bloomington, IN 47408

EXO-200 is an experiment searching for neutrinoless double beta decay using a time projection chamber with 175 kg of liquid xenon enriched in ^{136}Xe. The observation of this process would indicate that the neutrino is a Majorana fermion and lepton number is not a conserved quantity, and would allow for the calculation of the absolute mass of the neutrino. The low radioactive background and high sensitivity of the experiment also provide a venue to search for other theoretical exotic processes. Majoron modes of double beta decay are processes that would occur if a scalar boson is created in the neutrino self interaction, resulting in an electron sum spectral shape that deviates from the standard two-neutrino double beta decay spectrum. With two years of livetime, an exposure of 99.8 kg·yr to ^{136}Xe was collected, and a stringent limit on the half-life of neutrinoless double beta decay of $T_{1/2}^{0\nu\beta\beta} > 1.1 \cdot 10^{25}$ yrs (90% C.L.) was set. Lower limits on the half-lives of the Majoron-emitting processes are presented, and the future of the experiment is discussed.

1 Why Search for Neutrinoless Double Beta Decay?

Double beta decay is a second-order weak process that only occurs in certain even-even nuclei where single beta decay is energetically forbidden, or forbidden by conservation of angular momentum. Double beta decay has been observed in 11 nuclei, including ^{136}Xe, which undergoes the process $^{136}_{54}\mathrm{Xe} \rightarrow {}^{136}_{56}\mathrm{Ba}^{++} + 2\mathrm{e}^- + 2\bar{\nu}_\mathrm{e}$. The EXO-200 (Enriched Xenon Observatory) experiment has done a precision measurement of the half-life of two-neutrino double beta decay ($2\nu\beta\beta$) in ^{136}Xe, with $\mathrm{T}_{1/2}^{2\nu\beta\beta} = 2.165 \pm 0.016(\mathrm{stat}) \pm 0.059(\mathrm{sys}) \cdot 10^{21}$ years [1].

An isotope that undergoes the process of $2\nu\beta\beta$ is a candidate for the theoretical process of neutrinoless double beta decay ($0\nu\beta\beta$). In the $0\nu\beta\beta$ process, no anti-neutrinos are emitted in the decay ($^{136}_{54}\mathrm{Xe} \rightarrow {}^{136}_{56}\mathrm{Ba}^{++} + 2\mathrm{e}^-$). The observation of $0\nu\beta\beta$ has the potential to answer important lingering questions about neutrinos:

- *Is the neutrino of Dirac or Majorana nature?* Neutrinos are the only observed fundamental particles that have the potential to be of a Majorana nature, fermions with ν and $\bar{\nu}$ differing only by chirality. Neutrinos are candidates because they are observed to be massive [2], are electrically neutral, and all observations have been consistent with ν_L and $\bar{\nu}_R$ handedness [4]. If neutrinos are of a Dirac nature, ν and $\bar{\nu}$ are distinct, following the nature of all other Standard Model fermions. $0\nu\beta\beta$ can only occur in the Majorona case, if one of the anti-neutrinos participating in the double beta decay process undergoes a virtual spin-flip to cancel the other anti-neutrino, as shown in Figure 1.

- *What is the absolute mass of the neutrino?* Neutrinos have been observed to exist in three mass-states, with the square of the mass-state differences measured by neutrino oscillation experiments[5,6]. However, the absolute masses are yet unknown, as is the exact ordering of the masses. Two orderings are possible; they are known as the normal and inverted hierarchies.

Figure 1 – Feynman diagrams of $2\nu\beta\beta$ (left) and $0\nu\beta\beta$ (right) [3].

A measurement of the half-life of $0\nu\beta\beta$ would allow the calculation of an effective Majorona mass from the relation $(T^{0\nu}_{1/2})^{-1} = G^{0\nu}(Q,Z)|M^{0\nu}|^2\langle m_{\beta\beta}\rangle^2$, where $G^{0\nu}(Q,Z)$ is a calculable phase space factor and $|M^{0\nu}|$ is the nuclear matrix element. $\langle m_{\beta\beta}\rangle$ is the effective Majorona mass, which can be used to calculate the value of the lowest mass-state. Depending on the value of $\langle m_{\beta\beta}\rangle$, the mass hierarchy can also be resolved.

- *Is Lepton number a conserved quantity?* In all experiments performed to date, Lepton number (l) has always been conserved (with $l_{e^-} = 1$ and $l_{\bar{\nu}_e} = -1$). The overall process of $0\nu\beta\beta$ violates l by two counts, which would prove that l is not a conserved quantity.

There also exist alternative models of neutrinoless double beta decay in which a new particle (or two) called a Majoron is created in addition to the two betas [7]. The Majoron particle (χ_0) must be a chargeless scalar boson to comply with conservation quantities, with the decay process becoming $^{136}_{54}\mathrm{Xe} \rightarrow {}^{136}_{56}\mathrm{Ba}^{++} + 2\mathrm{e}^- + \chi_0(2\chi_0)$. Multiple theories exist for the nature of the particles, whether 1 or 2 χ_0 particles are emitted, if they are Goldstone Bosons, and by what value l is violated. For each of these theories, a spectral index n is defined that governs the spectral shape of the $0\nu\beta\beta\chi_0(\chi_0)$ decay, with $\frac{d\Gamma}{d\epsilon_1 d\epsilon_2} \propto (Q - \epsilon_1 - \epsilon_2)^n$, where $d\Gamma$ is the differential decay rate, ϵ_i is the kinetic energy of the ith electron, and Q is the Q-value of the double beta decay, the energy difference between the mother and daughter isotope.

2 How to search for $0\nu\beta\beta$?

A standard $2\nu\beta\beta$ will share the energy of the Q-value between the two emitted electrons and anti-neutrinos. This energy sharing is what provides the spectrum of summed electron energies emitted in a double beta decay, with the endpoint at the Q-value, shown in green on the left image in Figure 2. If no anti-neutrinos are emitted in the decay, the sum of the emitted electron energies will be exactly the Q-value. An experiment which measures the energy of electrons from double beta decay has the potential to measure this energy peak from a known $2\nu\beta\beta$ isotope. Good energy resolution is required to resolve the $0\nu\beta\beta$ peak (shown in purple in the left plot in Figure 2) from the $2\nu\beta\beta$ spectrum, and an in-depth knowledge of all backgrounds to the experiment is required as the process is expected to be extremely rare.

A Majoron mode decay would emit an extra particle, so there would not be a peak at the standard $2\nu\beta\beta$ endpoint. Instead, the standard $2\nu\beta\beta$ spectral shape would be altered. The raw spectra for each Majoron mode that was searched for in EXO-200 are shown on the right plot in Figure 2.

3 The EXO-200 Experiment

The EXO-200 experiment uses 175 kg of liquid xenon enriched to 80.6% in the isotope ^{136}Xe to search for neutrinoless double beta decay. ^{136}Xe has the advantage of a high Q-value of 2458 keV

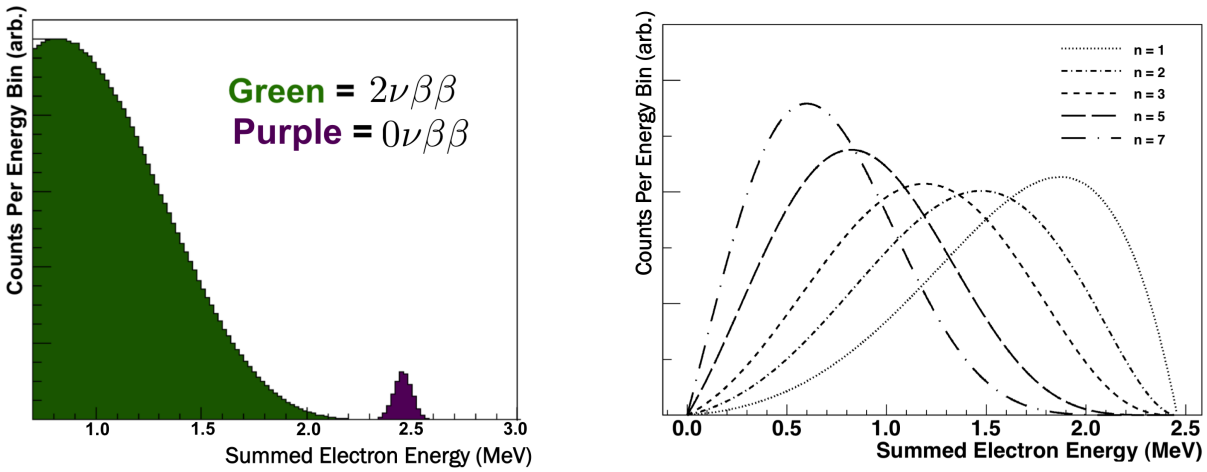

Figure 2 – The left figure shows the electron sum spectrum for $2\nu\beta\beta$ of ^{136}Xe in green, with a peak representing theoretical $0\nu\beta\beta$ in purple. The figure assumes a finite detector energy resolution. A good energy resolution will improve the ability to detect $0\nu\beta\beta$ over the $2\nu\beta\beta$ signal. The right plot shows the raw energy spectrum of each Majoron mode that is searched for with EXO-200. The n=5 mode represents the standard $2\nu\beta\beta$.

[8], above many of the gamma lines from common natural radioactive isotopes. The exceptions, and important radioactive backgrounds to understand, come from the ^{232}Th and ^{238}U decay chains. The xenon is self shielding and attenuates outside gamma radiation, reducing backgrounds and allowing for discrimination of backgrounds based on detector position. There are no long-lived radio-isotopes of xenon, although ^{137}Xe is cosmogenically activated through neutron capture and acts as a background to the experiment. Xenon scintillates at 178 nm through partial recombination of ionization electrons with the ionized xenon. Both ionization and scintillation channels are detected in the experiment.

The detector consists of two back-to-back cylindrical time projection chambers (TPCs) that share a central mesh cathode biased to 8 kV [9]. Each TPC is roughly 20 cm in radius and 22 cm in length. Scintillation light from electron recombination is reflected from teflon tiles surrounding the cylindrical barrel and is collected on a plane of Large-Area Avalanche Photodiodes (APDs) at each TPC end-cap. The free ionization electrons are drifted under the influence of an electric field between the central cathode and anodes at each end-cap. The anode of each TPC is a plane of stretched phosphor-bronze wires held at virtual ground, where the free electrons are collected. Another plane of wires set 6 mm in front of the anode plane and crossed at 60° from the anode plane detects an induction signal as the electrons pass. The combination of the immediate scintillation signal and delayed ionization signals provides a full 3-dimensional event position reconstruction.

The detector is housed under an overburden of 1585 meters water equivalent at the Waste Isolation Pilot Plant near Carlsbad, NM, USA. The module housing the detector is surrounded on four sides by scintillating muon veto panels, which are used to reject events occurring near a muon signal. The TPC is surrounded on all sides by 25 cm of lead, 5 cm of copper, and at least 50 cm of HFE-7000 cryofluid to shield from outside radiation, and all materials placed near the detector have been specially selected for low radioactivity. The xenon is continually circulated through a system that heats it into the gas phase and subjects it to a series of purifiers to remove electronegative impurities.

4 Analysis Techniques

The detector is calibrated with multiple external radioactive sources, with gamma lines covering the full relevant energy spectrum. The main calibration source is ^{228}Th, with a gamma line at 2.6 MeV from ^{208}Tl. This gamma line, close to the ^{136}Xe Q-value, is used to find the optimal combination of ionization and scintillation signals to minimize the energy resolution.

A detailed simulation of the detector setup has been constructed in Geant4 [12], and this is used

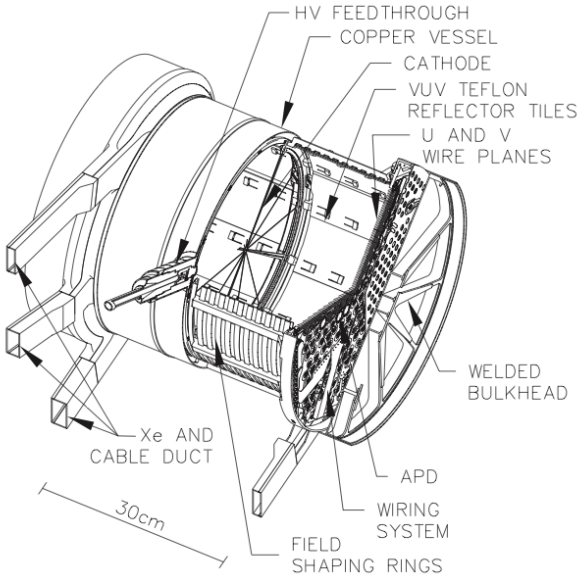

Figure 3 – Cutaway view of the TPC showing the copper vessel, cathode and anodes (u-wire planes), APDs, high voltage feedthrough, teflon reflector, biased rings that shape the electric field, and ducts for LXe and wiring through the mounting legs.

to simulate all signal and backgrounds that are expected to contribute to the data. The output from these simulations are subjected to similar data selection cuts as the data and smeared with the energy resolution determined from source calibration data to make probability distribution functions (PDFs). The PDFs are 2-dimensional, with observables of energy and "stand-off distance," or the distance between a charge signal and the closest detector component. PDFs are fit to histograms of the selected data with a negative log likelihood function to measure the relative contributions of each signal and background component. PDFs are fit to the source calibration data to determine the analysis threshold, data corrections, and various systematic errors.

The data are separated into categories of single-site (SS) and multi-site (MS) depending on whether one or more separate charge deposits are detected in a single event. This provides gamma background discrimination as most beta events are SS, while gamma events tend to Compton scatter, leaving multiple separate charge deposits in the detector. The measured MS events constrain the contributions of different backgrounds to the SS spectrum.

5 Results

Data for these analyses were collected between September 22, 2011 and September 1, 2013. After cuts to data due to quality and muon vetos, the livetime for the analysis is 477.60 ± 0.01 days. Using a hexagonal prism fiducial volume with a apothem of 162 mm in the x-y plane and $10 < |z| < 182$ mm results in an exposure to ^{136}Xe of 99.8 kg·yr.

5.1 $0\nu\beta\beta$ Search

For the search for $0\nu\beta\beta$, a PDF was made for the $0\nu\beta\beta$ mode and fit alongside the various backgrounds. The PDFs in the model were fit to the selected data in both SS and MS channels with a negative log likelihood function (left plot of Figure 4). The best fit value for a profile over the $0\nu\beta\beta$ mode was ~ 10 counts, but this result is consistent with zero at the 90% confidence level (C.L.), so a lower limit of $T_{1/2}^{0\nu\beta\beta} > 1.1 \cdot 10^{25}$ yrs is claimed [13].

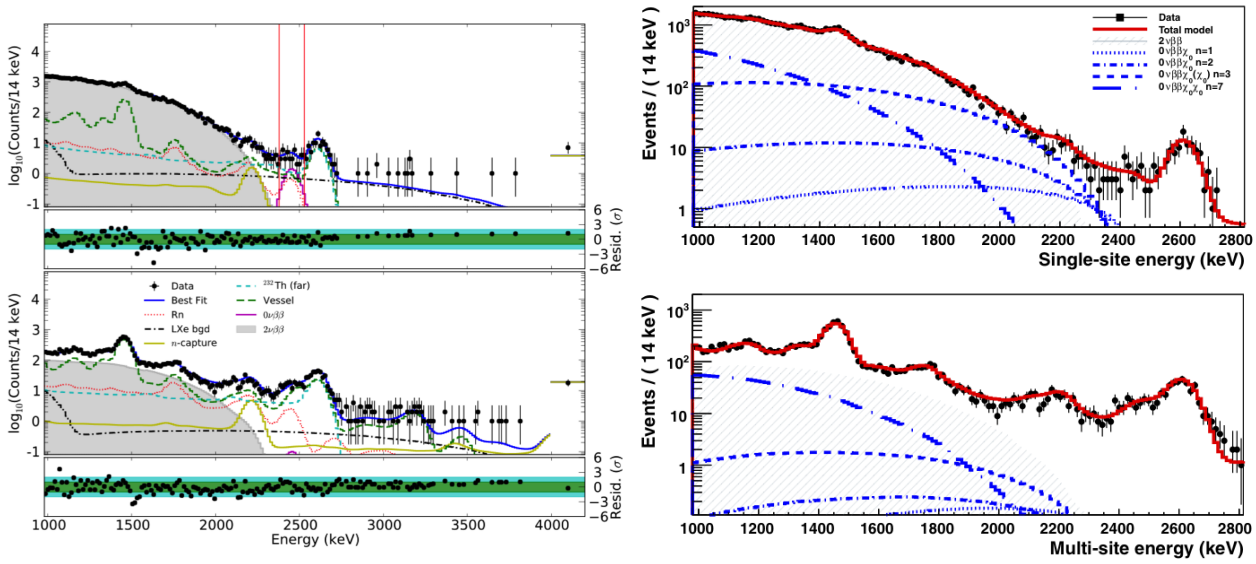

Figure 4 – The left plot shows the SS (upper) and MS (lower) fitted spectra for the $0\nu\beta\beta$ search. The colored lines represent the background groups added to the fit model, and the grey represents the fit to $2\nu\beta\beta$. The $\pm 2\sigma$ region of interest in SS is highlighted in red, showing the best fit PDF for $0\nu\beta\beta$. The right plot shows the best fit model (red line) for the fit to data (black points) with the n=1 Majoron mode included at the 90% C.L. The 90% C.L. fits to each of the other Majoron modes that were searched for are superimposed on the plot to illustrate the magnitude of each mode.

5.2 Majoron Mode Search

Majoron modes for indices 1, 2, 3, and 7 were all searched for separately, assuming no inclusion of the standard $0\nu\beta\beta$ mono-energetic peak. The PDF for each mode was fit alongside the background model, and the number of counts for each mode was profiled over to get the lower half-life limit at the 90% C.L. [14]. These half-life limits were used to set limits on the Majoron-neutrino couplings ($|\langle g_{ee}^{M} \rangle|$) for each mode, shown in Table 1. The right plot in Figure 4 shows the signal + background model fit (red line) over the data (black dots) for the 90% C.L. n=1 Majoron mode search, with the hatched section representing the fit to the $2\nu\beta\beta$. The three other modes that were searched for are superimposed onto the figure to show the magnitudes of the fit to each mode.

Table 1: The half-life lower limits at the 90% C.L. are shown for each Majoron mode that was searched for, along with the limits on the Majoron-neutrino couplings. The spread in the couplings is due to the uncertainty in matrix elements [15,16,17].

Decay Mode	Spectral Index, n	$T_{1/2}$, yr	$\lvert\langle g_{ee}^{M} \rangle\rvert$
$0\nu\beta\beta\chi_0$	1	$> 1.2 \cdot 10^{24}$	$< (0.8 - 1.7) \cdot 10^{-5}$
$0\nu\beta\beta\chi_0$	2	$> 2.5 \cdot 10^{23}$	—
$0\nu\beta\beta\chi_0\chi_0$	3	$> 2.7 \cdot 10^{22}$	$< (0.6 - 5.5)$
$0\nu\beta\beta\chi_0$	3	$> 2.7 \cdot 10^{22}$	< 0.06
$0\nu\beta\beta\chi_0\chi_0$	7	$> 6.1 \cdot 10^{21}$	$< (0.5 - 4.7)$

6 Conclusions and Future Outlook

The EXO-200 detector has proved to be a high sensitivity probe of physics beyond the Standard Model. Stringent limits have been set for the half-lives of both $0\nu\beta\beta$ and Majoron modes with indices 1, 2, 3, and 7. The null results are in agreement with the KamLAND-Zen experiment [10, 11]. The EXO-200 detector is expected to take more data with improved electronics and further background reduction, increasing sensitivity to $0\nu\beta\beta$. As the sensitivity to $0\nu\beta\beta$ is proportional to the source mass and inversely proportional to the background counts and resolution [18], a new

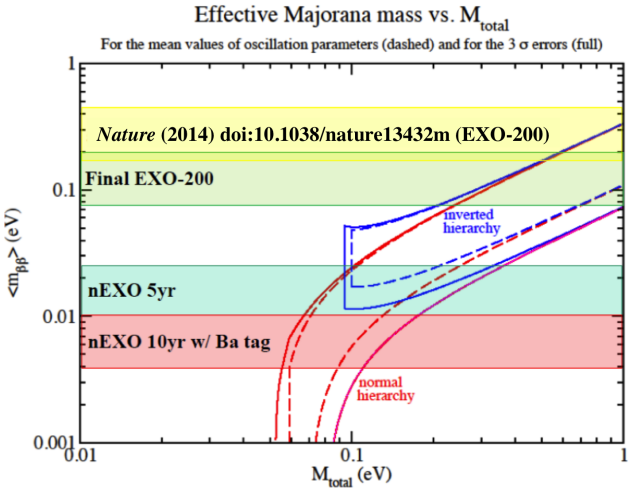

Figure 5 – This plot shows the sensitivity to the effective Majorana mass of the neutrino (calculated from the half-life of $0\nu\beta\beta$) against the sum of neutrino masses. The sensitivity of the nEXO 5-year plan will probe the inverted mass hierarchy, with the band width attributed to the matrix element calculation. The upgrade of nEXO with barium tagging could cover the inverted hierarchy and probe into the normal hierarchy.

detector that uses the knowledge gained through the running of EXO-200 with increased mass could greatly increase the physics reach on a reasonable time scale. A next-generation detector called "nEXO" is being planned that will use approximately 5 tonnes of enriched liquid xenon. The current research and development shows that the nEXO detector will have a sensitivity great enough to probe the inverted mass hierarchy after five years of run-time, and probe into the normal hierarchy after ten years with the upgrade of a barium tagging technique, where the daughter ^{136}Ba ion is positively identified, allowing rejection of nearly all backgrounds.

References

1. J. B. Albert *et al.* [EXO-200 Collaboration], Phys. Rev. C **89**, no. 1, 015502 (2014).
2. Y. Fukuda *et al.* [Super-Kamiokande Collaboration], Phys. Rev. Lett. **81**, 1562 (1998).
3. F.T. Avignone III et al., Double Beta Decay, Majorana Neutrinos, and Neutrino Mass, arxiv:0708.1033v2 [nucl-ex] (2007).
4. Wu, C. S.; Ambler, E.; Hayward, R. W.; Hoppes, D. D.; Hudson, R. P. (1957).
5. T. Araki *et al.* [KamLAND Collaboration], Phys. Rev. Lett. **94**, 081801 (2005).
6. D. G. Michael *et al.* [MINOS Collaboration], Phys. Rev. Lett. **97**, 191801 (2006).
7. P. Bamert, C. P. Burgess and R. N. Mohapatra, Nucl. Phys. B **449**, 25 (1995).
8. M. Redshaw, E. Wingfield, J. McDaniel, and E. G. My- ers, Phys. Rev. Lett., 98, 053003 (2007).
9. M. Auger, D. J. Auty, P. S. Barbeau, L. Bartoszek, E. Baussan, E. Beauchamp, C. Benitez-Medina and M. Breidenbach *et al.*, JINST **7**, P05010 (2012).
10. A. Gando *et al.* [KamLAND-Zen Collaboration], Phys. Rev. Lett. **110**, no. 6, 062502 (2013).
11. A. Gando *et al.* [KamLAND-Zen Collaboration], Phys. Rev. C **86**, 021601 (2012).
12. J. Allison, K. Amako, J. Apostolakis, et al., IEEE Trans. Nucl. Sci., 53, 270 (2006), ISSN 0018-9499.
13. J. B. Albert *et al.* [EXO-200 Collaboration], Nature **510**, 229 (2014).
14. J. B. Albert *et al.* [EXO-200 Collaboration], Phys. Rev. D **90**, no. 9, 092004 (2014).
15. J. Menendez, A. Poves, E. Caurier and F. Nowacki, Nucl. Phys. A **818**, 139 (2009).
16. F. Simkovic, A. Faessler, H. Muther, V. Rodin and M. Stauf, Phys. Rev. C **79**, 055501 (2009).
17. M. Hirsch, H. V. Klapdor-Kleingrothaus, S. G. Kovalenko and H. Pas, Phys. Lett. B **372**, 8 (1996).
18. S. R. Elliott and P. Vogel, Ann. Rev. Nucl. Part. Sci. **52**, 115 (2002)